

MS No. S-2017-376.R1

Controlling Mass Concrete Effects in Large-Diameter Drilled Shafts Using Full-Length Central Void

by Gray Mullins, Kevin R. Johnson, and Danny Winters

Mass concrete defines elements where heat formation due to exothermic hydration reactions can induce tension cracking as a result of excessive temperature differentials upon cooling. These conditions are anticipated in dams, large footings, and, in some cases, pier columns and caps where internal cooling systems can be used to moderate the effects. Until 2006, drilled shafts were not recognized by the Florida Department of Transportation as mass concrete due to the relatively small diameters (4 ft [1.2 m] diameter being the most common) and/or the perception that the surrounding environment was not conducive to producing mass concrete conditions. This paper presents the results of a full-scale shaft demonstration project where a 9 ft (2.74 m) diameter shaft was constructed with a 3.8 ft (1.17 m) diameter central void to control temperature and reduce costs. Peak and differential temperatures were shown to stay well within specified limits without the need for internal cooling systems.

Keywords: differential temperature; drilled shaft; mass concrete; peak temperature; voided shaft.

INTRODUCTION

The term “mass concrete” gives the connotation of being a large or massive concrete element and generally that is true. The Florida Department of Transportation (FDOT)¹ uses the American Concrete Institute (ACI)² definition for mass concrete: “any large volume of cast-in-place or precast concrete with dimensions large enough to require that measures be taken to cope with the generation of heat and attendant volume change so as to minimize cracking.” Starting in 1994, FDOT adopted the ACI differential temperature limit as a means to reduce the probability of thermal-induced cracking; in 2010, guidelines for peak internal core temperature were added.³ These specifications state peak and differential temperatures must stay below thresholds of 180 and 35°F (82°C and 19°C), respectively.⁴ As mixture designs vary (for example, slag cement replacement mixtures produce lower internal temperatures), the shape and size can have a lesser effect than binder type and content. Therefore, in reality, mass concrete is not a size but a state of internal temperature (magnitude and distribution).

Upper limits for concrete core temperature stem from the concerns associated with delayed ettringite formation (DEF), which occurs at elevated curing temperatures. This reaction may lay dormant for several years before occurring or may not occur at all, as it depends on numerous variables involving the concrete constituent properties and environment. Concrete mixtures with low pozzolan levels have lower threshold temperatures, whereas higher pozzolan content concretes may not exhibit adverse effects

up to 185°F (85°C).⁵ FDOT assigned a slightly lower limit at 180°F (82°C) based on this research.

Differential temperature limits are imposed to prevent internal stresses that accompany concrete that cures at varying rates from the temperature distribution within the element. As core temperatures are higher than edge temperatures, the center-most concrete will undergo more thermal contraction and induce tension in early-age, relatively low-strength concrete. Strength gain is linked to time and curing temperature, so non-uniform strength and modulus distributions ensue within an element, making the quantification of an appropriate differential temperature limit difficult. Further, the size of the element (temperature gradient) will affect the ability to withstand tensile forces resulting from a given temperature change.

The traditional approach of predicting when mass concrete conditions might occur is to evaluate the volume-to-area ratio. Therein, any concrete element with volume in cubic feet greater than the dissipative surface area in square feet would likely be unable to stay within reasonable temperature limits. Further, if the minimum dimension of a concrete element is 3 ft (0.91 m) or greater, the same lack of temperature control can be anticipated.^{1-4,6} Criteria for the identification of mass concrete have evolved and continue to do so with a more complete understanding.

Today, large-diameter drilled shafts are routinely constructed that qualify as mass concrete elements by all criteria. This presents more complications to an already difficult construction process where cooling tubes are incorporated into the reinforcing cage, making tremie access difficult. Figure 1 shows a 7 ft (2.13 m) diameter cage for an 8 ft (2.44 m) diameter shaft congested with cooling tubes to combat mass concrete conditions.

This paper describes a cost-saving, temperature-controlling measure where large-diameter shafts are cast with a full-length central void. The method removes the need for cooling systems and reduces the total quantity of concrete.

RESEARCH SIGNIFICANCE

To date, the true magnitude of an acceptable differential temperature limit in concrete is unknown. Presently, the same temperature limits are applied to large or small elements

ACI Structural Journal, V. 115, No. 5, September 2018.

MS No. S-2017-376.R1, doi: 10.14359/51702376, was received October 3, 2017, and reviewed under Institute publication policies. Copyright © 2018, American Concrete Institute. All rights reserved, including the making of copies unless permission is obtained from the copyright proprietors. Pertinent discussion including author's closure, if any, will be published ten months from this journal's date if the discussion is received within four months of the paper's print publication.



Fig. 1—Tubes in shaft cage required to circulate coolant.

without knowledge of the actual stresses that develop or the acceptable stress levels for maturation-dependent concrete strength and modulus. While peak concrete core temperature must also stay below a safe threshold, differential temperature limits often control. The findings of this study provide compelling evidence in favor of using voided shaft construction where possible to remove many of the uncertainties that plague mass concrete effects by reducing all internal temperatures to inarguably acceptable levels.

BACKGROUND

In 2002, the Ringling Causeway Bridge in Sarasota, FL, was approved for construction with large-diameter shafts (9 ft [2.74m]) but also raised concerns that perhaps shafts had been slipping through the mass concrete specifications without review. These were not the first large shafts to be constructed in Florida, but some of the first scrutinized for mass concrete conditions. Temperature measurements from within the center of shaft and cage locations showed, in fact, mass concrete conditions were exhibited (Fig. 2).

More recently, results from thermal integrity profiles show that the temperature gradient in the cover of drilled shafts is typically 4 to 5°F/in. (0.9 to 1.1°C/cm), making the true core to edge differential up to 30°F (16.7°C) higher than that normally measured between the core and reinforcement cage.^{7,8} Therefore, it is highly likely that most shafts have core-to-edge differential temperatures that exceed all published criteria. If added to the measured 67°F (37°C) differential at the Ringling Causeway Bridge, the actual or probable differential temperature was more likely closer to 97°F (54°C).

In the absence of quantifiable values for mass concrete effects in shafts, FDOT assigned a size limit of 6 ft (1.83 m) diameter (based on experiences with Ringling Bridge) to delineate when mass concrete specifications should be considered. However, using the simplistic volume/area ratio, the shaft cutoff diameter should have been a bit more restrictive, limiting it to 4 ft (1.22 m) diameter shafts, as shown in Fig. 3. This graph implies that longer shafts are less able to dissipate heat as the volume/area ratio increases with length. Thermal integrity results indicate that the mid-length

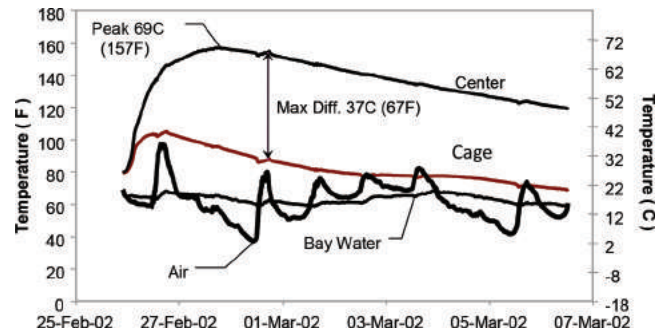


Fig. 2—Temperature traces from Ringling Causeway Bridge.⁹

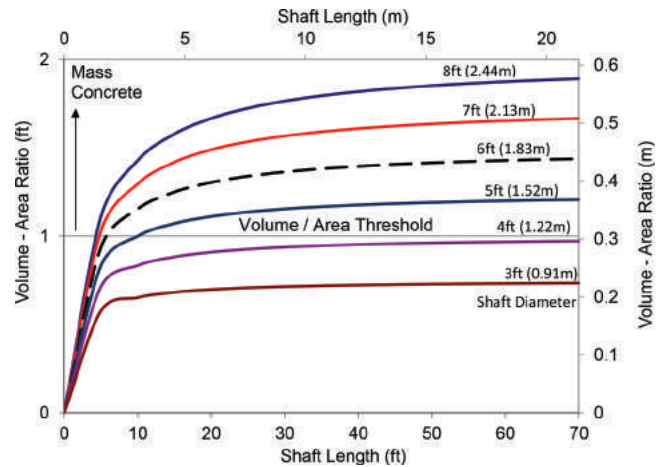


Fig. 3—Mass concrete geometry criteria applied to various shaft diameters.

internal temperature distribution (radially) does not get any warmer for shaft lengths greater than two diameters. This distance is time-dependent, starting at a zero length and increasing proportional to the square root of time but never extends farther than one diameter from each end at times of peak temperature.⁷

Shafts with diameters of 2 ft (0.61 m) were shown to exceed differential temperature limits for mass concrete⁹; and shafts as small as 4 ft (1.22 m) in diameter can exceed peak temperature limits.¹⁰ In those studies, the differential from 2 ft (0.61 m) shafts was based on model results calibrated with field tests and where the true shaft edge temperature was used instead of cage-based measurements. The 4 ft (1.22 m) diameter core temperature was measured in a shaft cast in saturated sands using a FDOT-approved shaft mixture.¹¹

These somewhat startling findings led in part to an innovative construction process whereby mass concrete conditions can be averted by casting shafts with a full-length central void (cast-in-place cylinder pile). This paper extends the hypothetical voided shaft concept introduced by Johnson and Mullins⁹ and presents the results from a 9 ft (2.74 m) diameter shaft cast with a 3.8 ft (1.17 m) diameter central void for the express purpose of mitigating mass concrete temperature distributions in large-diameter drilled shafts. Focus is given to the construction, field measurements, and numerical model calibration. Complete details of the entire study can be found in Mullins et al.¹⁰

PRACTICAL CONSIDERATIONS

When considering the use of voided shafts, several topics arise: temperature control, strength, durability, constructability, and cost. Reviews of the temperature components are presented. The other four were thoroughly vetted by Johnson and Mullins,⁹ but are simply summarized.

Strength

The axial capacity is reduced proportional to the cross-sectional area of void concrete removed, but axial capacity of drilled shafts is rarely the issue; bending moments from lateral extreme events more often control. Large prestressed piles (2 to 3 ft [0.6 to 0.9 m]) can be cast with a cylindrical void aligned with the longitudinal axis of the pile to minimize construction weight while also reducing concrete cost. Larger-diameter post-tensioned cylinder piles (3 to 6 ft [0.9 to 1.8 m]) develop enormous axial and bending capacity with only a 6 to 8 in. (15 to 20 cm) thick annular ring of concrete (concrete pipe pile). A voided shaft is an even larger version, where only a small reduction in bending capacity was shown to occur.⁹ Geotechnically, there is no loss in side shear surface area when using voided shafts, and end bearing of large-diameter shafts rarely contributes significantly to the capacity due to strain compatibility.¹²

Durability

The durability of voided shafts is no different than conventional, non-voided shafts where the outer concrete cover protecting the reinforcing steel is still the same. The distance between the reinforcing cage and the inner void surface should also be maintained to provide sufficient protection, and constructability issues nullify this concern.

Constructability

An inner casing (permanent or removable) must be provided to hold back the fluid concrete as it is placed and cures. The casing must form a sufficient seal to prevent concrete intrusion from the toe of the casing. Buoyancy of the voided region/casing does not develop, as no bottom surface is available for the fluid concrete to press upward, and drill slurry is left in place; again, review Johnson and Mullins.⁹ The radial distance between the cage and central casing should be left as large as practical to promote concrete flow around the casing (for example, 1.5 ft [0.5 m] minimum). Use of multiple tremies may also be adopted depending on site access.

Cost

The introduction of a central casing has associated costs that are offset by the reduction in concrete volume and removal of an internal cooling system. Unit costs for these items vary, but the break-even analysis presented by Johnson and Mullins⁹ showed that even when not considering the savings from omitting cooling systems, the casing cost versus the reduction in concrete cost of the void were about the same at a void diameter of 4 ft (1.12 m) and became more cost effective with larger-diameter voids.

VOIDED SHAFT CONSTRUCTION

The logistics of constructing a voided shaft were addressed in a full-scale demonstration project conducted as part of the study. This was made possible in part with the cooperation of a local drilled shaft contractor who provided a site, personnel, and equipment. A thorough review of the construction process and the effectiveness in controlling mass concrete effects in large-diameter drilled shafts is presented.

The shaft size was selected to replicate the Ringling Causeway Bridge (9 ft [2.74 m] diameter), but the length (25 ft [7.6 m]) was set based on numerical modeling that indicated that the shaft length needed to be at least two times the diameter (18 ft [5.5 m]). This ensured that the worst-case, mid-length radial temperature distribution would not be affected by end conditions. The same Class IV shaft mixture that caused peak core temperatures in a 4 ft (1.22 m) shaft to exceed mass concrete limits¹¹ was intentionally used.

The reinforcement cage consisted of 36 longitudinal bars and nine 2 in. (51 mm) Schedule 80 polyvinyl chloride (PVC) integrity access tubes equally distributed inside 93 in. (2.36 m) diameter No. 5 stirrups spaced at 12 in. (0.3 m). Thermocouple wires were attached to three of the access tubes (120 degrees apart) at the top, middle, and bottom of the tubes. The central casing was 30.5 ft (9.3 m) long, 3.8 ft (1.17 m) OD, and had a 1/2 in. (13 mm) wall thickness. Thermocouple wires were tied to steel nuts welded down the length of the central casing both on the inside and outside. An additional access tube was centered within the central casing using radial struts welded to the inside.

Access tubes were also installed in the ground around the shaft at distances $D/4$, $D/2$, $1D$, and $2D$ from the edge of shaft to monitor ground temperature effects, where D represents the shaft diameter. Thermocouples were attached to the soil access tubes at the middepth of the shaft (12.5 ft [3.8 m] depth).

The excavation was stabilized using polymer slurry and an 8 ft (2.44 m) long, 10 ft (3 m) diameter temporary surface casing. A 9 ft (2.74 m) diameter, double-flight, double-cutting dirt auger on a truck-mounted drill rig was used to excavate the silty, sandy soils. Excavation, cleanout, and cage placement procedures were the same as a conventional non-voided shaft. After the cage was installed and suspended by beams spanning the temporary casing, the 3.8 ft (1.17 m) diameter casing was installed by hanging it plumb, centered within the excavation and seating it approximately 6 in. (15 cm) into the underlying soil. While more sophisticated methods could be adopted to secure the top of casing, the contractor opted to simply hold the central casing with a backhoe for the remainder of the construction process.

Concreting was performed with two tremies on opposite sides of the central casing and where two concrete trucks could access the tremie hoppers. Standard, Class IV FDOT shaft mixture (4000 psi [28 MPa]) was used with an 8 in. (20 cm) slump and 1 in. (25.4 mm) maximum coarse aggregate. This mixture had 708 lb/yd³ (246 kg/m³) of total cementitious material with 20% Type F fly ash. During concrete placement, the concrete level at three points around the shaft was measured to ensure concrete was flowing around the central void uniformly and through the reinforcing cage into



Fig. 4—Excavation and cleanout.



Fig. 5—Cage placement.

the cover region. The temporary casing was removed using two boom trucks. Figures 4 through 9 show the entire voided shaft construction sequence.

POST-CONSTRUCTION EVALUATION

Twenty-five thermocouples located within the shaft, central casing, and surrounding soil were connected to a data acquisition system capable of uploading information to the university website at 15-minute intervals. Data were collected for several months and uploaded for review

as part of a separate study assessing remote monitoring systems for bridges.¹³ The data are archived on the same site: <http://geotech.eng.usf.edu/Voided.html>. The information includes time-lapse photography of the construction, thermocouple data, and sample thermal integrity profiles from the shaft and soil access tubes. Figure 10 shows the temperature traces from selected shaft and soil locations at middepth. The highest recorded temperature was 139°F (59°C) and the highest measured differential (Fig. 11) was approximately 29°F (16°C). The true shaft/soil interface temperature was



Fig. 6—Central casing installation.



Fig. 7—Central casing installation and held in-place with backhoe bucket.

not measured, but all shaft and soil temperature traces were used to signal match the measured temperatures with numerical models.

NUMERICAL MODELING

The results from selected locations in and around the voided test shaft were used to calibrate a numerical model and extend the findings to an array of various shaft sizes and wall thicknesses. The model input parameters included cement and fly ash constituents from mill certifications,

mixture design proportions, density, thermal conductivity, and physical dimensions (Table 1). The Table 1 parameters were used in all models and represent the concrete mixture used in the voided shaft demonstration.

Finite difference models were run using multi-physics software where a special hydration energy evolution module was created based on Schindler and Folliard¹⁴ using the mill certs and mixture design information (Table 1). Thermal conductivity values were taken from literature for saturated silty sand¹⁵⁻¹⁷ and concrete.^{14,18} Model results shown



Fig. 8—Concreting with two tremies on opposite sides of central casing.



Fig. 9—Surface casing extraction and final shaft (permanent void casing).

in Fig. 12 represent the middepth temperature distribution across a 9 ft (2.74 m) diameter voided and non-voided shaft. The field-measured temperatures just inside the inner casing and at the cage are also shown and verify the model calibration. The modeled peak temperature of 143°F (61.3°C) was 3.7°F (1.3°C) higher than that measured at the location of the cage in the field (139°F [60°C]) and occurred at the center of

the concrete annulus (approximately equidistant from edge of shaft and inner casing). The modeled concrete/soil interface temperature (112°F [44.4°C]) was similar in magnitude but slightly lower than the central casing temperature (118°F [47.8°C]), making the highest differential temperature 31°F (10.8°C) from model results. Peak field differential temperature was 29°F (16°C).

Table 1—Numerical model input parameters

Cement	318 kg/m ³ (536 lb/yd ³)	Fly ash	79.4 kg/m ³ (134 lb/yd ³)	Sat. soil den.	2000 kg/m ³ (125 lb/ft ³)
MgO	0.8%	SO ₃	3.1%	Specific heat	1500 J/kg-K (0.36 Btu/lb-°F)
C ₂ S	14%	CaO	2.54%	Therm. cond.	2.2 W/m-K (1.3 Btu/h-ft-°F)
C ₃ A	7%	Concrete density	2231 kg/m ³ (3760 lb/yd ³)	Slurry density	1100 kg/m ³ (68.7 lb/ft ³)
C ₃ S	59%	w/c	0.41	Specific heat	3600 J/kg-K (0.89 Btu/lb-°F)
Blaine	393 m ² /kg (1923 ft ² /lb)	Specific energy	73 kJ/kg (31 Btu/lb)	Therm. cond.	0.8 W/m-K (0.46 Btu/h-ft-°F)
SO ₃	3.1%	Specific heat*	1144 J/kg-K (0.273 Btu/lb-°F)	Air, concrete, and slurry temperature	28°C (82°F)
C ₄ AF	11%	Thermal conductivity*	3.58 W/m-K (2.07 Btu/h-ft-°F)	Soil temperature	23°C (73°F)

*Initial values only. The relationships for thermal conductivity and specific heat of concrete throughout hydration can be found in Reference 14.

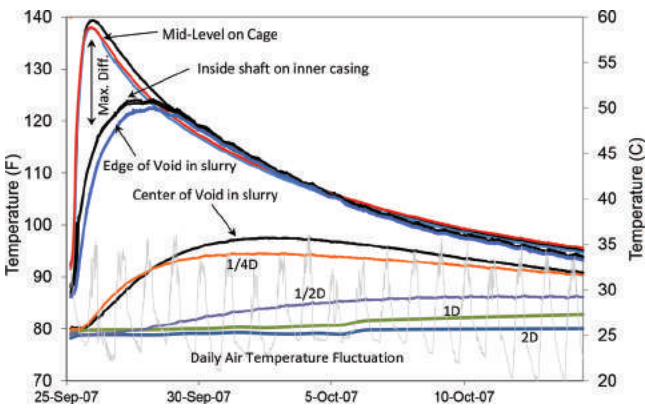


Fig. 10—Temperature data from voided shaft and surrounding soil.

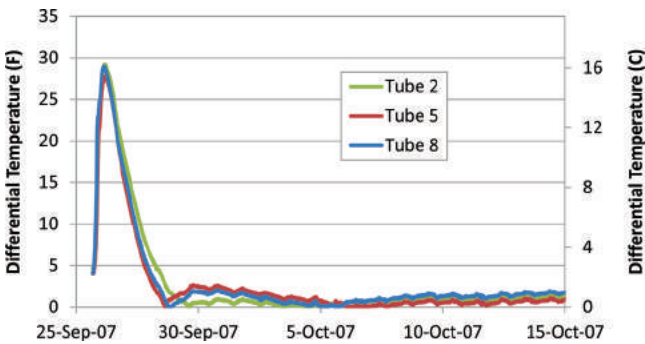


Fig. 11—Differential temperature versus time.

For the non-voided shaft, the modeled peak core temperature was 171.4°F (77.4°C) and the highest differential temperature was 54.4°F (30.2°C). The peak core temperature for the voided and non-voided shafts occurred at significantly different times of 18 and 38 hours, respectively.

Using the calibrated model, a series of different shaft sizes and concrete wall thicknesses were evaluated to identify trends for optimized design or construction considerations. A practical limit of 1.5 ft (0.46 m) minimum wall thickness was imposed based on 6 in. (150 mm) cover, 2 in. (51 mm) cage thickness, and the remainder for a small pump truck tremie. The range of wall thicknesses was also constrained by the full radius of the shaft size, which corresponds to a non-voided shaft. Figure 13 shows the resulting peak temperatures and the 180°F (82°C) peak temperature is

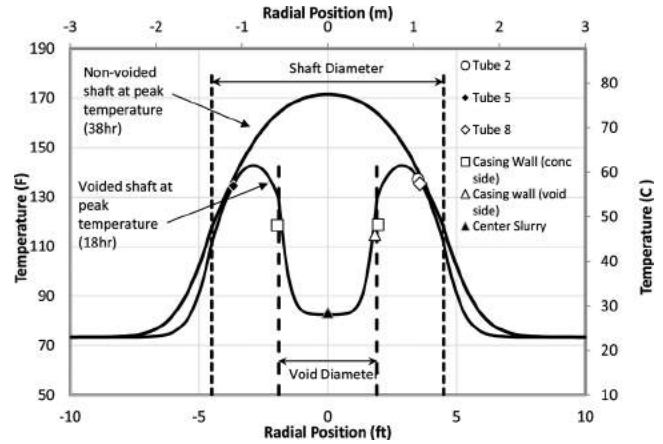


Fig. 12—Model temperature distributions with measured data.

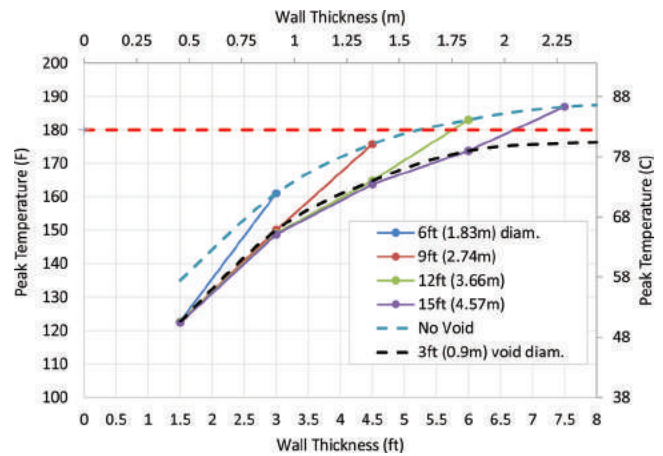


Fig. 13—Peak internal temperature for various shaft/void configurations.

exceeded when non-voided shafts were larger than 9 ft (2.74 m) in diameter. Figure 14 shows the highest differential temperature that occurs for the same shaft size and wall thickness configurations. The differential temperature limit of 35°F (19°C, dashed horizontal line) intersects each of the shaft size/wall thickness curves at the limiting dimensions for voided shafts that will not exceed differential limits. This also suggests that a 3.6 ft (1.1 m) diameter non-voided shaft will not exceed either temperature limit. Figure 15 shows a range of acceptable void diameters that satisfy differential

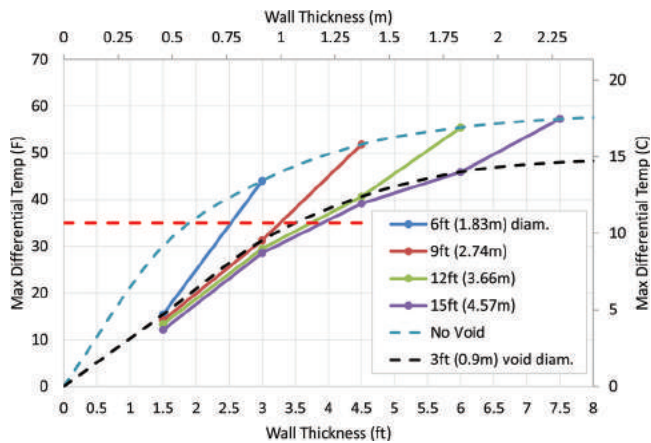


Fig. 14—Highest differential temperature for various shaft/void configurations.

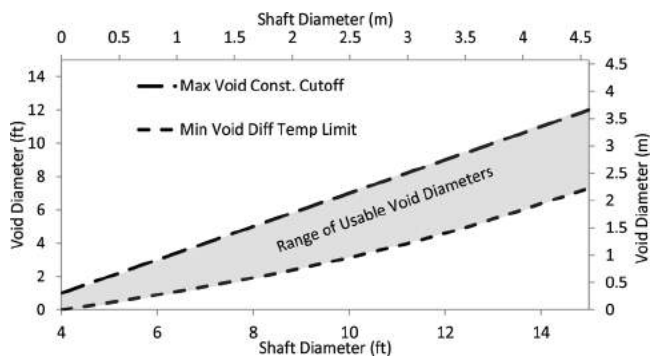


Fig. 15—Range of usable void diameters that satisfy both mass concrete and constructability considerations.

temperature limits as well as construction limitations assuming a minimum 1.5 ft (0.46 m) wall thickness. The field demonstration used 10 in. (0.25 m) diam. pipes, so a wider 2.5 ft (0.76 m) nominal wall thickness was selected. It should be noted that the differential temperature limit, and not the peak temperature limit, controlled in all modeled configurations.

DISCUSSION

While the rationale for limiting the upper permissible temperature is well defined based on DEF potential, the true magnitude of a permissible differential temperature is vague and should be linked to the concrete tensile strength, the coefficient of thermal expansion, and element geometry. However, this is complicated by strength gain being mix and curing temperature dependent, where the concrete at the center of the shaft experiences higher temperature and hence faster maturation. High-early-strength mixtures capable of developing significant strength while the concrete is still cooling are accompanied by higher heat energy production and internal temperature from the associated increase in cement content.

Methods to mitigate peak or differential temperatures such as use of ice water or chilled aggregates are effective² but require additional cost and/or logistics, especially in warmer climates. Use of high percentages of slag cement replacement is also an alternative, but often delays subsequent

construction due to slow strength gain. Hence, great expense and effort go into mitigating mass concrete conditions with cooling systems that, for shafts, introduce cage congestion and complications associated with providing adequate tremie access. Use of voided shafts is simple, cost-effective, easily designable, and removes the logistical issues noted herein.

CONCLUSIONS

This study showed that use of a central void in drilled shafts was constructible and eliminated mass concrete temperature conditions. The worst-case measured differential temperature was below the acceptable limit where the true edge temperature was used (not just the cage location). Numerical models calibrated with the measured temperatures were used to provide a range of acceptable void diameters (wall thicknesses) that would prevent mass concrete effects. In short, a voided shaft with wall thickness between 2 and 3 ft (0.6 and 0.9 m) was shown to not exceed mass concrete temperature limits using a relatively high-energy shaft concrete mixture.

DISCLOSURE

This technology was developed by the University of South Florida, for which the author is an active researcher and faculty member. As is customary with such developments, the principal investigator was named as one of the inventors.¹⁹

AUTHOR BIOS

ACI member **Gray Mullins** is a Professor in the Department of Civil and Environmental Engineering at the University of South Florida, Tampa, FL, where he received his BS, MS, and PhD. His research interests include foundation design, construction, and quality assurance.

Kevin Johnson is a Postdoctoral Researcher at the Department of Civil and Environmental Engineering at the University of South Florida, where he received his BS, MS and PhD in civil engineering. His research interests include post-tensioned splices for prestressed piles, thermal integrity analysis of drilled shafts, and use of self-consolidating concrete in drilled shafts.

Danny Winters is a Senior Geotechnical Engineer with Foundations & Geotechnical Engineering, LLC, Plant City, FL. He received his BS, MS, and PhD in civil engineering from the University of South Florida. His research interests include development of underwater fiber-reinforced polymer repair methods for corrosion-damaged concrete piles, methods for making thermal integrity measurements, and software development used to analyze piles tested by rapid load test methods.

ACKNOWLEDGMENTS

The authors would like to thank R. Harris and C. Harris from R.W. Harris, Inc. for their continued support that made this construction/demonstration possible. The authors also acknowledge the Florida Department of Transportation for funding the original study. The opinions, findings, and conclusions expressed in this publication are those of the authors and not necessarily those of the Florida Department of Transportation or the U.S. Department of Transportation.

REFERENCES

1. FDOT, "Structures Design Guidelines," FDOT Structures Manual, Volume 1, Section 1.4.4, Mass Concrete," Florida Department of Transportation, Tallahassee, FL, 2017.
2. ACI Committee 207, "Guide to Mass Concrete (ACI 207.1R-05) (Reapproved 2012)," American Concrete Institute, Farmington Hills, MI, 2012, 30 pp.
3. FDOT, "Standard Specifications for Road and Bridge Construction, Section 346-3.3 Mass Concrete," Florida Department of Transportation, Tallahassee, FL, 2010.

4. FDOT, "Standard Specifications for Road and Bridge Construction, Section 346-3.3 Mass Concrete," Florida Department of Transportation, Tallahassee, FL, 2017.
5. Whitfield, T. T., "Effect of C₃S Content on Expansion Due to Ettringite Formation," master's thesis, University of South Florida, Tampa, FL, 2006.
6. FDOT, "Structures Design Guidelines, Section 3.9, Mass Concrete," Florida Department of Transportation, Tallahassee, FL, 2007.
7. Johnson, K. R., "Temperature Prediction Modeling and Thermal Integrity Profiling of Drilled Shafts," *Proceedings from ASCE Geo-Congress*, V. 2014, 2014, pp. 1781-1794. doi: 10.1061/9780784413272.175
8. Mullins, G., "Thermal Integrity Profiling of Drilled Shaft," *DFI Journal*, V. 4, No. 2, Dec. 2010, pp. 54-64. doi: 10.1179/dfi.2010.010
9. Johnson, K. M., and Mullins, G., "Concrete Temperature Control via Voiding Drilled Shafts," *Contemporary Issues in Deep Foundations*, ASCE Geo Institute, GSP, V. I, No. 158, 2007, pp. 1-12.
10. Mullins, G.; Winters, D.; and Johnson, K. M., "Attenuating Mass Concrete Effects in Drilled Shafts," *Final Report*, FDOT Project BD-544-39, Sept. 2009, 148 pp.
11. Mullins, G., and Kranc, S., "Thermal Integrity Testing," *Final Report*, FDOT Project BD544-20, Dec. 2007, 214 pp.
12. AASHTO, "LRFD Bridge Design Specifications, U.S. Customary Units, seventh edition 2014 with interim revisions thru 2016," American Association of State Highway and Transportation Officials, Washington, DC, 2010.
13. Mullins, G.; Winters, D.; and Collins, J., "Foundation Health Monitoring," Final Report submitted to FHWA, June 2009, 334 pp.
14. Schindler, A. K., and Folliard, K. J., "Temperature Control During Construction to Improve the Long Term Performance of Portland Cement Concrete Pavements," Center for Transportation Research. The University of Texas at Austin, Austin, TX, 2004.
15. Farouki, O., "Physical Properties of Granular Materials with Reference to Thermal Resistivity," *Highway Research Record 128*, National Research Council, Washington, DC, 1966, pp. 25-44
16. Johansen, O., "Thermal Conductivity of Soils," U.S. Army Corps of Engineers Cold Regions Research and Engineering Laboratory, Hanover, NH, 1977, pp. 1-46
17. Kersten, M. S., "Thermal Properties of Soils," University of Minnesota Institute of Technology, Engineering Experiment Station, Vol. LII, No. 21, 1949.
18. Mindess, S.; Young, J.; and Darwin, D., *Concrete*, second edition, Prentice Hall, Pearson Education, Inc., Upper Saddle River, NJ, 2003.
19. Mullins, G., and Johnson, K., "Voided Drilled Shafts" U.S. Patent No. 8,206,064 B2, 2012.

NOTES:
